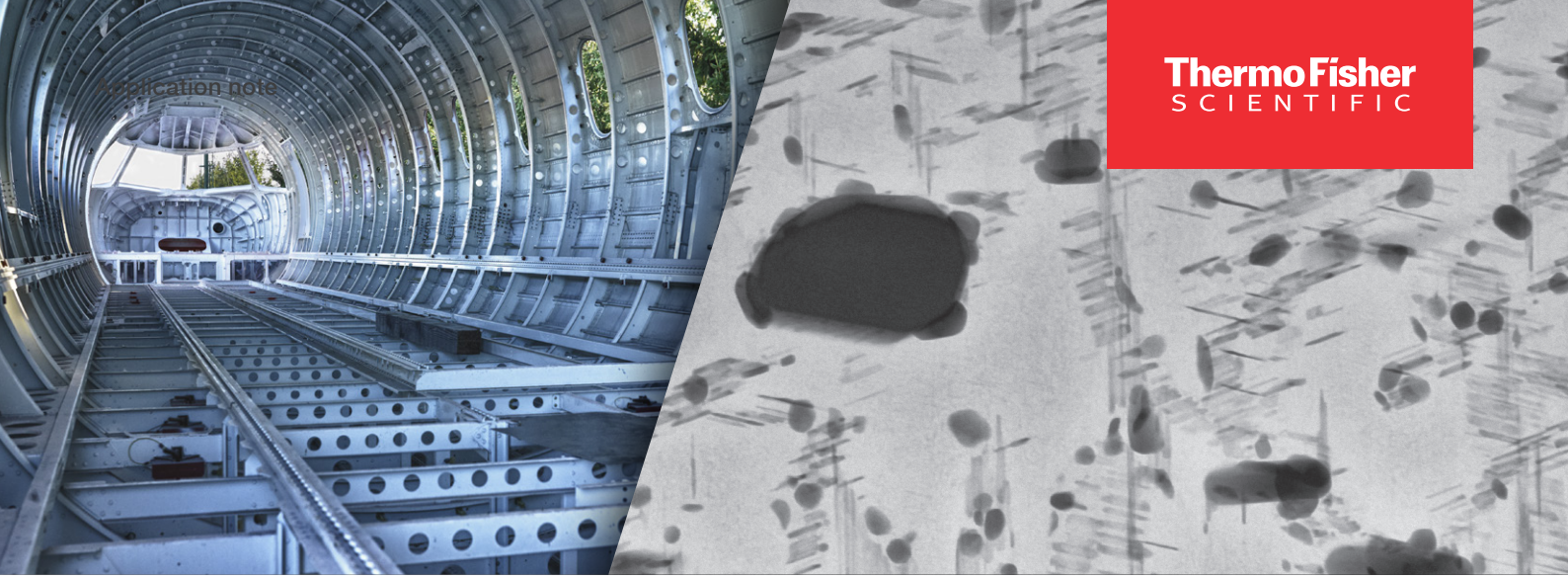

Application note

Microstructural characterization of aging-treated aluminum alloy AA2024

Comprehensive analysis of precipitates, dispersoids, and microstructure with SEM, STEM, EDS, and EBSD

Authors

Alice Scarpellini, Roger Maddalena, and Chris Stephens, Thermo Fisher Scientific

Introduction

The rapid development of the aerospace industry has created significant demand for materials with enhanced strength, toughness, and corrosion resistance. Aluminum alloys, specifically 2xxx-series alloys such as AA2024, are widely used in various components due to their light weight and resistance to corrosion. While primarily used by the aircraft industry for structural aircraft parts, AA2024 is also found in truck wheels, gears, and orthopedic equipment.

To further enhance these materials, additional alloying elements are introduced to improve their mechanical, physical, and chemical properties, as well as their processing capabilities like formability, workability, and sintering response. The selection and quantity of alloying elements depend on the desired properties and applications. In the case of AA2024, the main alloying elements are copper and magnesium, with a small amount of manganese.

The presence of these alloying elements leads to the formation of precipitates, whose type varies based on the applied treatments. Therefore, it is crucial to comprehensively characterize raw materials during the manufacturing process, revealing the compositional and microstructural evolution of the alloy under different treatments such as aging, hardening, or annealing. This application note presents a detailed characterization of three AA2024 samples subjected to different aging treatments. Characterization consisted of scanning electron microscopy (SEM), scanning transmission electron microscopy (STEM), energy dispersive spectroscopy (EDS), and electron backscatter diffraction (EBSD).

Together, these methods were used to identify and analyze precipitates, intermetallic particles, and dispersoids, while also enabling compositional comparison across the three samples. EBSD was used to determine grain structure and orientation, which was then correlated to EDS data.

The Thermo Scientific™ Apreo™ ChemiSEM facilitated the acquisition and processing of this comprehensive data through integrated Thermo Scientific™ ChemiSEM™ Technology and a streamlined EBSD workflow, providing smooth and efficient analysis.

Microscale characterization with SEM-EDS

The table below shows the compositional range of the AA2024 alloy used in this study.

Element	Concentration (weight %)
Si	0–0.5
Cr	0–0.1
Cu	3.8–4.9
Mg	1.2–1.8
Mn	0.3–0.9
Fe	0–0.5
Zn	0–0.25
Ti	0–0.2
Al	Balance

thermo scientific

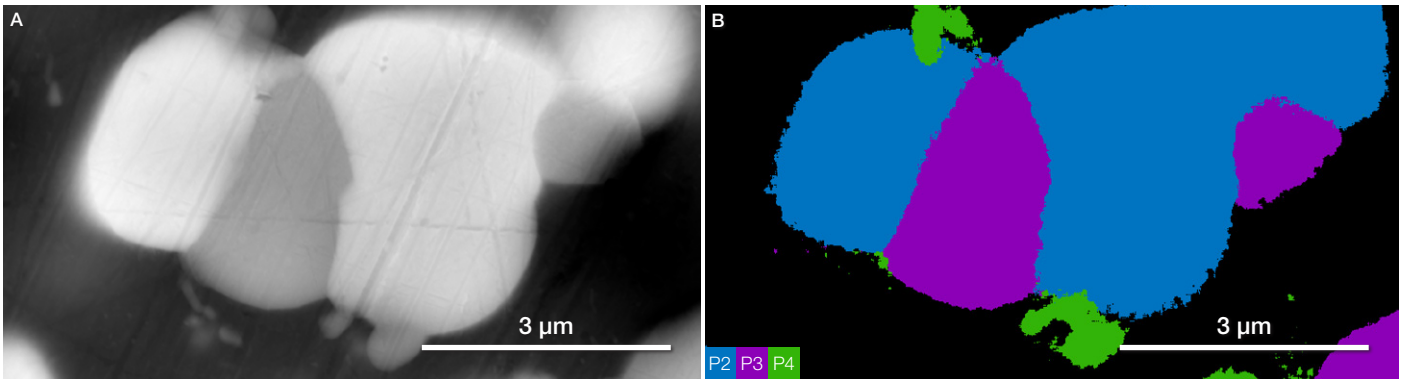

	P2: θ phase	P3: S phase	P4
Element	**Atomic %**	**Atomic %**	**Atomic %**
Al	75.3	68.2	82.9
Cu	21.4	19.4	11.4
Fe	-	-	1.0
Mn	0.1	0.1	0.4
Mg	3.0	12.1	4.0
Ni	0.2	0.2	0.3

Figure 1. AA2024 sample subjected to the T3 aging treatment. Various intermetallic particles are differentiated through a combination of backscattered electron contrast imaging (A) and ChemiPhase analysis (B). Different colors in the ChemiPhase map represent distinct phases. (The phase related to the base alloy has been hidden to focus on the intermetallic particles.) The table shows quantification of the observed phases; compounds identified in the literature have been easily assigned to specific intermetallic particles.

The base material was subjected to different treatments, with the sequence, strength, and type of treatment heavily affecting the types of precipitates that formed:

- T3: Heat treated, cold rolled, then naturally aged to a substantially stable condition
- T6: Heat treated then artificially aged
- T81: Heat treated, cold rolled, then artificially aged

The type of precipitates, intermetallic particles, and dispersoids formed in AA2024 are well documented in the literature.[1-2] Some of the most common types are listed below to contextualize the subsequent analyses presented in this application note. Note that all the possible dispersoids and precipitates are not exhaustively classified, as these can vary significantly depending on the treatment.

- S phase (Al_2CuMg) particles, with a Mg/Cu atomic ratio between 0.63 and 1.0
- θ phase (Al_2Cu) particles, with a Mg/Cu atomic ratio between 0.10 and 0.26
- α phase (AlCuFeMn(Si)) particles, with compositional ranges of 55–65 wt% Al, 10–20 wt% Fe, 6–12 wt% Cu, 5–10 wt% Mn, and 0–5 wt% Si
- T phase ($Al_{20}Mn_3Cu_2$) nanoscale dispersoids, showing a varying stoichiometry of 60–70 wt% Al, 15–25 wt% Mn, and 10–20 wt% Cu

The morphology, type, and distribution of the analyzed particles were characterized with ChemiPhase analysis on the Apreo ChemiSEM. ChemiPhase is an automated and real-time phase analysis component of ChemiSEM Technology that efficiently provides all the information needed for fast and comprehensive particle characterization.

Figure 1 shows a variety of microscale intermetallic particles in the AA2024-T3 sample. Material contrast in the backscattered electron (BSE) images was used to distinguish particles with different physical characteristics. Conventional EDS analysis confirmed the presence of varying ratios of Cu, Mn, Mg, and Fe in all these particles, but was not able to conclusively determine the types of precipitates and the area fraction of each type. Automated ChemiPhase analysis, meanwhile, was able to identify all the materials present in the analyzed area. ChemiPhase assigns each material to a specific phase and automatically calculates the associated spectrum, quantification, and area fraction. Based on literature values, the light blue and purple phases could be attributed to the θ and S phase respectively. It is notable that particle aggregation and/or fusion would make precise compositional analysis of these particles challenging with EDS alone.

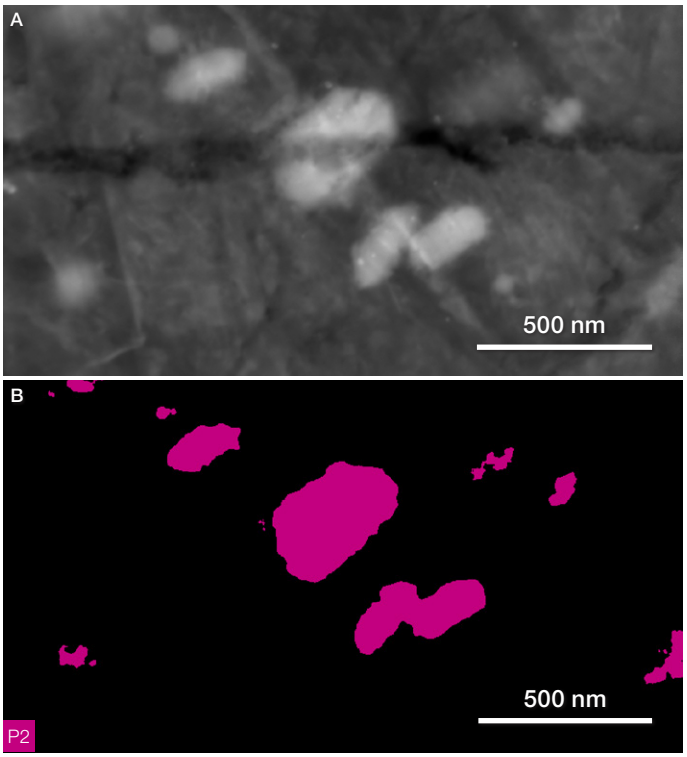

	P2: T phase
Element	**Atomic %**
Al	91.4
Cu	3.6
Mg	1.6
Mn	3.4

Figure 2. AA2024 sample subjected to the T6 aging treatment. The BSE contrast image (A), together with the ChemiPhase map (B), highlights the formation of nanoscale dispersoids. The table shows the quantification extracted from the ChemiPhase analysis.

Figure 2 indicates that a number of T-phase nanoscale dispersoids formed during T6 aging treatment; these are known to enhance the strength of aluminum alloys.[4] Their average size ranges from 0.05 µm to 0.5 µm. Further characterization of these dispersoids, in all the different heat-treated samples, will be presented later in this application note.

Figure 3 shows some of the intermetallic particles characterized in the T81 sample; these are seen throughout the matrix. While orange appears to indicate the familiar θ phase, the other particles, colored in purple, were not found in the other samples. Given their percent composition, they are likely σ phase particles with a composition of $Al_5Cu_6Mg_2$.[3]

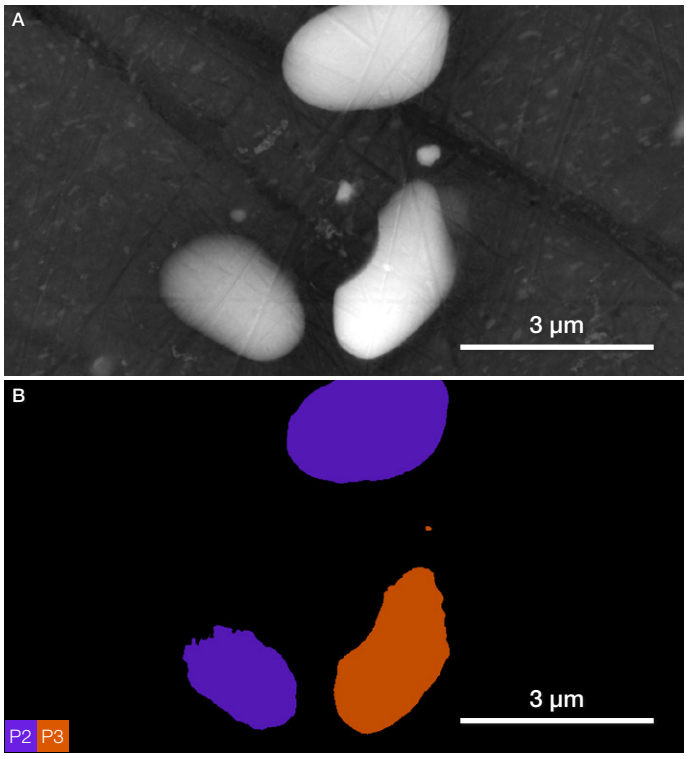

	P2: σ phase	P3: θ phase
Element	**Atomic %**	**Atomic %**
Al	85.6	89.3
Cu	8.0	8.4
Mg	5.9	1.6
Mn	0.3	0.3
Ni	0.2	0.4

Figure 3. AA2024 sample subjected to the T81 aging treatment. The BSE contrast image (A), together with the ChemiPhase map (B), show the formation of a unique precipitate.

Nanoscale characterization with STEM-EDS

The characterization of nanoscale features on the Apreo ChemiSEM has been enhanced with the retractable STEM 3+ detector, which offers scanning transmission imaging capabilities in various modes, including bright field, dark field, and high-angle annular dark field (HAADF). As ChemiSEM Technology is compatible with all available detectors, it can be combined with STEM analysis to characterize nanoscale dispersoids and assess differences across samples.

To perform the STEM imaging, transmission-thin lamellae were prepared from each AA2024 sample (T3, T6, T81) (Figure 4).

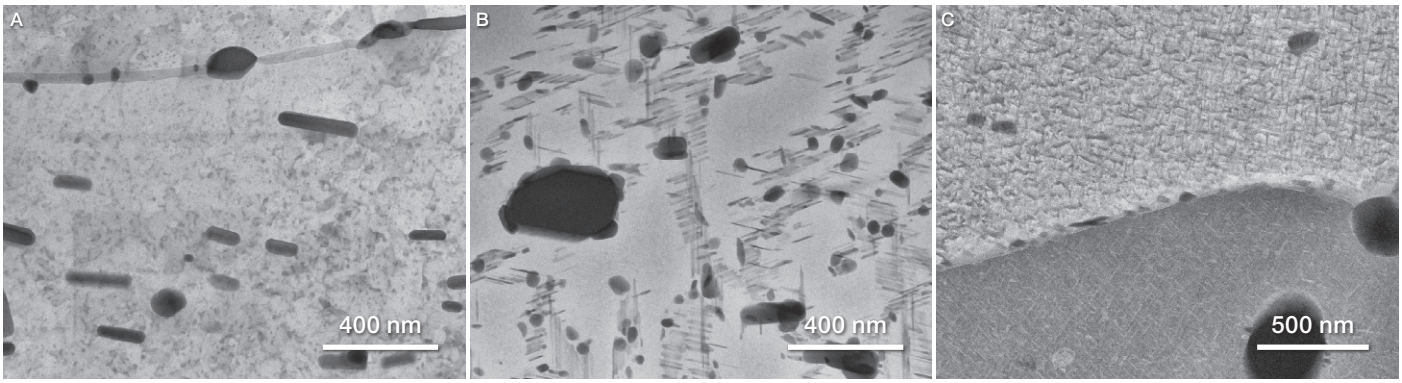

Figure 4. Low-magnification bright-field STEM images of the T3 (A), T6 (B), and T81 (C) alloy samples. Differences in dispersoid shape and size can clearly be seen.

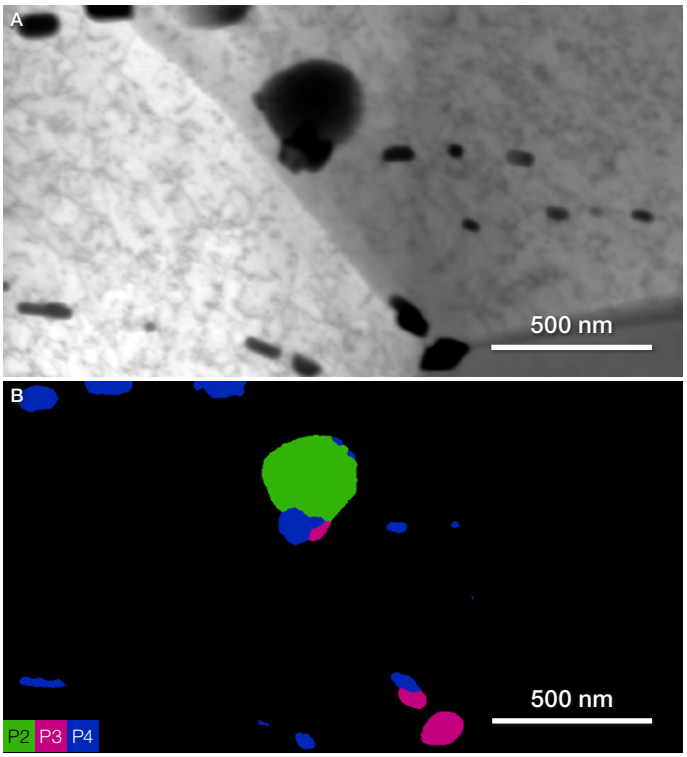

	P2: α phase	P3: θ phase	P4: T phase
Element	**Atomic %**	**Atomic %**	**Atomic %**
Al	84.2	85.8	89.5
Cu	4.7	13.7	6.6
Si	4.3	-	-
Mn	3.3	0.5	3.9
Mg	0.4	-	-
Fe	3.1	-	-

Figure 5. Bright field imaging (A) and ChemiPhase characterization (B) of nanoscale particles in the AA2024-T3 sample.

Figure 5 demonstrates the ChemiPhase characterization of the AA2024-T3 sample, confirming the presence of nanoscale particles that are likely α and θ phase, based on literature values.[5] Throughout the analyzed surface, these particles have largely been found along grain boundaries.

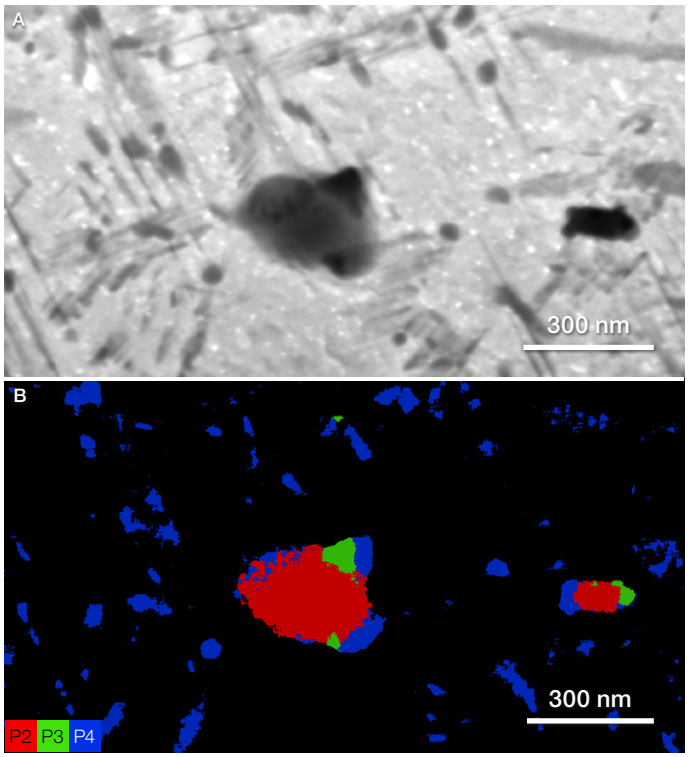

	P2: T phase	P3	P4
Element	**Atomic %**	**Atomic %**	**Atomic %**
Al	84.5	84.4	91.3
Cu	7.4	6.7	7.0
Si	0.7	-	-
Mn	7.0	3.6	0.5
Mg	0.4	5.3	1.2

Figure 6. Bright-field imaging (A) and ChemiPhase characterization (B) of dispersoids in the AA2024-T6 sample.

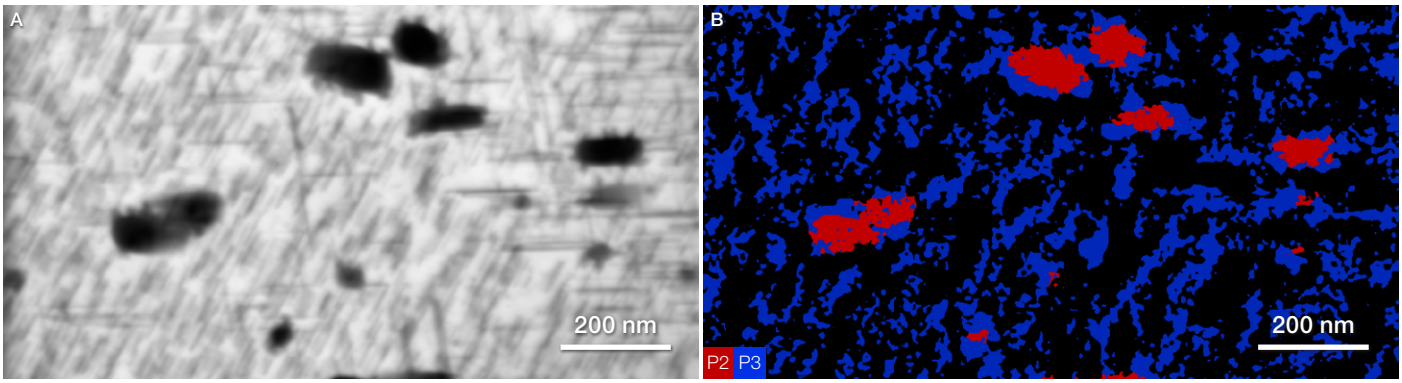

	P2: T phase	P3
Element	**Atomic %**	**Atomic %**
Al	86.4	92.5
Cu	6.8	4.9
Mn	5.4	0.3
Si	0.6	-
Mg	0.8	2.3

Figure 7. Bright-field imaging (A) and ChemiPhase characterization (B) of dispersoids in the AA2024-T81 sample.

The nanoscale EDS characterization of AA2024-T6 and AA202-T81 shows similar types of dispersoids across the 2 samples, but these differ in composition from those observed in AA2024-T3. The composition of the phase colored in red (Figure 6B and 7B) is comparable to T-phase dispersoids ($Al_{20}Mn_3Cu_2$) and features a rhomboidal shape that is consistent across the different samples. The other two phases, however, appear to be chemically different from any phases that were previously identified. They are, however, still composed of Al, Cu, Mn, and Mg, as is expected for nanoscale precipitates in these alloys.

Microstructural analysis with TruePix EBSD

EBSD provided further insight into the microstructure of the AA2024 aluminum alloy, yielding information on the crystallographic phase, grain orientation, grain structure, and morphology, as well as any material strain. Such details can be used to optimize heat treatment parameters in order to achieve desired mechanical properties and performance. To understand the effects of heat treatments on the alloy, three areas on each AA2024 sample (T3, T6, T81) were characterized, using the same experimental conditions, as shown in the following table.

Sample preparation	Mechanical polish to 250 µm followed by ion polish with the Thermo Scientific™ CleanMill™ Broad Ion Beam System
Accelerating voltage	20 kV
Probe current	6.4 nA
Step size	800 nm
Horizonal field of view	635 µm
Dwell time	1 ms
Frame rate	1000 FPS
Crystallographic phase	Aluminum Fm3m
Data clean up	Outlier removal

An SEM overview of the three samples is shown in Figure 8 (top), indicating a relatively similar distribution of intermetallic particles, and revealing some surface topography. (Particles appear brighter in the BSE images as they contain elements that are heavier than aluminum.) Inverse pole figure (IPF) orientation maps use different colors to represent crystallographic orientation, thereby clearly visualizing the differences between the three heat treatments (Figure 8, bottom). The T3 and T81 samples display large and relatively uniform grains, with average sizes of 480 ± 50 μm^2 and 420 ± 70 μm^2, respectively. T6, which was not cold rolled, showed a much smaller grain size of 170 ± 90 μm^2. Corresponding IPF texture representations (not shown) indicated no significant texture. This uniformity was corroborated by KAM and misorientation angle plots, which showed no significant strain.

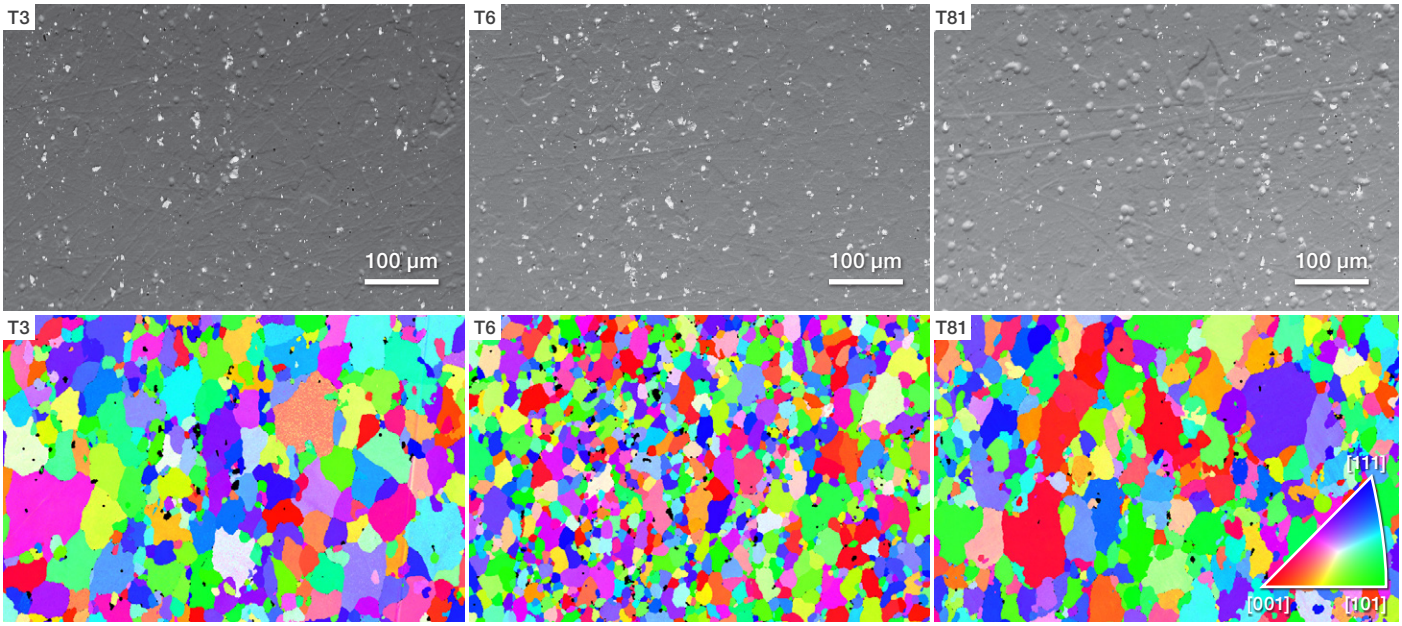

Figure 8. Top) Low-magnification BSE images showing the area of each sample that was analyzed with EBSD. Bottom) Inverse pole figure orientation maps reveal the different crystallographic orientations (X, Y, Z) of the grains.

Conclusions

Aluminum alloys, known for their light weight and corrosion resistance, are extensively used in aircraft and aerospace applications. Their superior mechanical properties and performance are derived from additional alloying elements, like copper and magnesium, which form various precipitates during treatments such as aging and hardening. Understanding the detailed composition and microstructure of these alloys is crucial to ensuring that final products meet aerospace standards and high-performance demands.

This application note presents a comprehensive characterization of three AA2024 aluminum alloy specimens subjected to different aging treatments. Analysis consisted of SEM, STEM, EDS, and EBSD, all performed within a single instrument, the Apreo ChemiSEM. This allowed for efficient and straightforward data acquisition and processing, facilitating the identification and comparison of precipitates, intermetallic particles, and dispersoids. The correlation of grain structure and orientation with EDS data provides the precise materials analysis needed by the ever-evolving aerospace industry.

References

1. DeRose, JA, *et al.* Localised corrosion initiation and microstructural characterisation of an Al 2024 alloy with a higher Cu to Mg ratio. *Corrosion Science* 55, p313–325 (2011). doi: 10.1016/j.corsci.2011.10.035
2. Zmywaczyk, J, et al. Investigation of Thermophysical Properties of AW-2024-T3 Bare and Clad Aluminum Alloys. *Materials* 13(15) p3345 (2020). doi: 10.3390/ma13153345
3. Barlow, IC, et al. The role of silicon in the formation of the ($Al5Cu_6Mg_2$) σ phase in Al-Cu-Mg alloys. *Journal of Materials Science* 35(6) p1413-1418 (2000). doi: 10.1023/a:1004767131956
4. S. Cheng, S, et al. Optimizing the strength and ductility of fine structured 2024 Al alloy by nano precipitation. *Acta Materialia* 55(17) p5822–5832 (2007). doi: j.actamat.2007.06.043
5. Xiao, X, et al. Microstructure and Its Effect on the Intergranular Corrosion Properties of 2024-T3 Aluminum Alloy. *Crystals* 12(3) p395 (2022). doi: 10.3390/cryst12030395

Learn more at **thermofisher.com/apreo-chemisem**

thermo scientific